Carotenoid-to-Chlorophyll Energy Transfer in Recombinant Major Light-Harvesting Complex (LHCII) of Higher Plants. I. Femtosecond Transient Absorption Measurements

Roberta Croce,* Marc G. Müller,* Roberto Bassi,† and Alfred R. Holzwarth*

*Max-Planck-Institut für Strahlenchemie, D-45470 Mülheim/Ruhr, Germany, and †Dipartimento Scientifico e Tecnologico, Facolta di Scienze, I-37134 Verona, Italy

ABSTRACT The energy transfer kinetics from carotenoids to chlorophylls and among chlorophylls has been measured by femtosecond transient absorption kinetics in a monomeric unit of the major light-harvesting complex (LHCII) from higher plants. The samples were reconstituted complexes with different carotenoid contents. The kinetics was measured both in the carotenoid absorption region and in the chlorophyll Q_y region using two different excitation wavelengths suitable for selective excitation of the carotenoids. Analysis of the data shows that the overwhelming part of the energy transfer from the carotenoids occurs directly from the initially excited S_2 state of the carotenoids. Only a small part (<20%) may possibly take an S_1 pathway. All the S_2 energy transfer from carotenoids to chlorophylls occurs with time constants <100 fs. We have been able to differentiate among the three carotenoids, two luteins and neoxanthin, which have transfer times of ~50 and 75 fs for the two luteins, and ~90 fs for neoxanthin. About 50% of the energy absorbed by carotenoids is initially transferred directly to chlorophyll b (Chl b), while the rest is transferred to Chl a. Neoxanthin almost exclusively transfers to Chl b. Due to various complex effects discussed in the paper, such as a specific coupling of Chl b and Chl a excited states, the percentage of direct Chl b transfer thus is somewhat lower than estimated by us previously for LHCII from *Arabidopsis thaliana*. (Connelly, J. P., M. G. Müller, R. Bassi, R. Croce, and A. R. Holzwarth. 1997. *Biochemistry.* 36:281). We can distinguish three different Chls b receiving energy directly from carotenoids. We propose as a new mechanism that the carotenoid-to-Chl b transfer occurs to a large part via the B_x state of Chl b and to the Q_x state, while the transfer to Chl a occurs only via the Q_x state. We find no compelling evidence in favor of a substantial S_1 transfer path of the carotenoids, although some transfer via the S_1 state of neoxanthin can not be entirely excluded. The S_1 lifetimes of the two luteins were determined to be 15 ps and 3.9 ps. A detailed quantitative analysis and kinetic model of the processes described here will be presented in a separate paper.

INTRODUCTION

The light-harvesting complex of photosystem II (LHCII) is the outermost and most abundant antenna complex of higher plants that binds the large majority of all chlorophyll (Chl) on earth. LHCII from maize binds 7 Chl a and 5 Chl b chromophores, and at least three carotenoids. Two of them are luteins, which occupy the central positions L1 and L2, while a third carotenoid is neoxanthin, which is located at a peripheral site (Croce et al., 1999a, b). The LHCII structure has been determined to near atomic resolution (3.4 Å) by electron microscopy (Kühlbrandt, 1994; Kühlbrandt et al., 1994). However, the information is not detailed enough to have a clear picture of the pigment orientation and assignment, and thus many questions as to the functional organization and pigment/protein coupling of this complex remain open. Answering these questions will be important for understanding several of the important functions of LHCII in the antenna systems of higher plant photosynthesis, such as adaptation to various light environments, photoinhibition, q_E-quenching, the role of carotenoids, etc. (Horton et al., 1996; Hankamer et al., 1997; Green and Durnford, 1996; Paulsen, 1995; Bassi et al., 1997).

Several previous attempts have been made to understand the structure/function relationships by time-resolved spectroscopy, both in fluorescence and in transient absorption, for LHCII and related complexes. These papers include the work from our own group (Cinque et al., 2000; Trinkunas et al., 1997, 1998; Connelly et al., 1997a, b), the Amsterdam group (Gradinaru et al., 1998; Kleima et al., 1997; Peterman et al., 1997b; Visser et al., 1996; Kwa et al., 1992; Savikhin et al., 1994), Fleming and co-workers (Du et al., 1994; Eads et al., 1987; Ide et al., 1986), and Wasielewski's group (Bittner et al., 1994, 1995). All this work has been devoted mostly to understanding the coupling and energy transfer among the Chls in the complex, and to a much smaller part to define the role of the carotenoids in the energy transfer pathways (Walla et al., 2000; Connelly et al., 1997a; Peterman et al., 1997b). Also, a great deal of steady-state and triplet spectroscopy has been performed (Barzda et al., 1998; Gülen et al., 1997; Peterman et al., 1995, 1996, 1997a; Nussberger et al., 1994). Several papers have been devoted primarily to elaborate modeling of the spectroscopic kinetic data on the basis of the known structure details (Gradinaru et al., 1998; Gülen et al., 1997; Visser et al., 1996; Trinkunas et al., 1997–1999; Valkunas et al., 1998, 1999). However, despite that substantial amount of work, no complete picture about the Chl organization, the

Received for publication 18 July 2000 and in final form 25 October 2000.

Address reprint requests to Dr. Alfred R. Holzwarth, Max-Planck-Institut für Strahlenchemie, Stiftstrasse 34, D-45470 Mülheim/Ruhr, Germany. Tel.: +49-208-3063571; Fax: +49-208-3063951; E-mail: holzwarth@mpi-muelheim.mpg.de.

0006-3495/01/02/901/15 $2.00

pigment-pigment coupling, and the functional role of the carotenoids has been obtained. Quite clearly, there are some problems achieving this goal that are caused on the one hand by the limited structure resolution available, and on the other hand by some surprising features of the pigment organization, which had not been anticipated. Thus it has now become clear that certain pigment binding sites do not differentiate strictly between Chl a and Chl b, and as a consequence certain sites in the LHCII family of antenna complexes, including the CP29 complex and others, feature mixed binding sites (Bassi et al., 1999; Giuffra et al., 1997; Remelli et al., 1999). Such a feature complicates the understanding of the spectroscopic data and their interpretation in a structural picture.

There now exists a general agreement between the different groups working in the field about the Chl-Chl energy transfer in the LHCII complex. At temperatures near room temperature the fastest Chl b-to-Chl a transfer seems to occur with a lifetime of ~150–200 fs. Further components have lifetimes of ~500–600 fs and 5–7 ps (Connelly et al., 1997b; Trinkunas et al., 1997; Kleima et al., 1997; Gradinaru et al., 1998). Energy transfer among the Chls a occur on a time scale typically 1 ps and longer (Trinkunas et al., 1997; Connelly et al., 1997b; Kleima et al., 1997; Visser et al., 1996).

A different approach, applying molecular genetics and reconstitution techniques, has been taken to gain insight into the structural organization of higher plant light-harvesting complexes, including LHCII (Plumley and Schmidt, 1987; Booth and Paulsen, 1996; Paulsen et al., 1993; Paulsen and Hobe, 1992; Giuffra et al., 1996, 1997). This has recently led to substantial progress, allowing in particular an assignment of the Chls in both the CP29 complex and the LHCII complex (Bassi et al., 1997, 1999; Simonetto et al., 1999; Sandona et al., 1998). This approach also allows reconstituting the pigment-protein complexes with different contents of pigments, and this possibility is exploited in the present paper as an important tool to further characterize the carotenoid-Chl interactions and energy transfer pathways. We present an extensive study of the femtosecond kinetics of the carotenoid-to-Chl and the Chl-Chl energy transfer in two reconstituted complexes of LHCII monomers containing a different carotenoid composition. Specifically, one sample contains only two luteins, while the other has a carotenoid content that is close to the wild type, i.e., two luteins in the central positions and a neoxanthin in the peripheral site (Croce et al., 1999a). By using different excitation wavelengths we attempt to excite the carotenoids in a different ratio in order to distinguish their kinetics and spectral contributions. The possibility of comparing the signals from these two samples turned out to be instrumental in arriving at a detailed kinetic model of the carotenoid-to-Chl transfer and to propose a specific location and spectral properties of the Chls in general, and of Chls b located in the vicinity of the carotenoids in particular. This is part of a diversified approach in our group to better understand the pigment organization and function in this antenna complex, using inter alia dimer modeling (Valkunas et al., 1999), kinetic modeling (Trinkunas et al., 1997–1999), and annihilation experiments (Müller et al., unpublished results).

In a previous paper reporting on a femtosecond study of the carotenoid-to-Chl energy transfer we concluded that in LHCII complexes isolated from *Arabidopsis thaliana* and one of its mutants, the carotenoid-to-Chl energy transfer occurred mainly via Chl b (in the wild type (w.t.) complex). This led us to suggest that several Chl b molecules must be located close to the central luteins in order to account for the very rapid lutein-to-Chl b energy transfer with a lifetime of ~120 fs (Connelly et al., 1997a). This finding was inconsistent with the previous pigment assignment (Kühlbrandt et al., 1994). In that work we were not able to distinguish the energy transfer contributions of the different luteins and/or the neoxanthin or violaxanthin molecules present in these complexes, however. A study of the Amsterdam group came to a quite different conclusion, i.e., that energy transfer from carotenoids to the Chls takes an overwhelming direct pathway to the Chls a (Peterman et al., 1997b). Although both papers implied preferential energy transfer from the S_2 state of the carotenoids to the Chls, a more recent study proposed that ~30% of the energy transferred to the Chls takes a path via the carotenoid S_1 state (Walla et al., 2000).

MATERIALS AND METHODS

The Lhcb1 expression system was previously described (Croce et al., 1999b). Plasmids were constructed using standard molecular cloning procedures and the bacterial host were *Escherichia coli* strains XL1Blue and SG13009. The LHCII apoprotein was isolated from the SG13009 strain transformed with the LHCII construct following a protocol described previously (Croce et al., 1999b). The procedures for reconstituting the LHCII-pigment complexes were performed as described (Croce et al., 1999b). Purification of the isolated complexes was performed by ion exchange chromatography, followed by ultracentrifugation in a glycerol gradient (15–40% including 0.06% β-dodecyl maltoside (DM) and 10 mM Hepes, pH 7.6; run was for 12 h at 60,000 rpm in a SW60 Beckman rotor) in order to eliminate the pigments unspecifically bound to the complex. The concentration of LHCII apoprotein purified from *E. coli* inclusion bodies was determined by the bicinconilic acid assay as described. Chlorophyll concentration was determined by the method of Porra (Porra et al., 1989). The carotenoid composition was analyzed by HPLC and the ratio between the pigments was checked by acetonic extract fitting (Connelly et al., 1997a). Absorption spectra were obtained using an SLM Aminco DW-2000 spectrophotometer at room temperature. Samples were in 10 mM Hepes, pH 7.6, 0.06% DM, 20% glycerol. The two samples bind 12 Chls each with a Chl a/b ratio of 1.6. For the LHCII-lutein sample only two luteins are present per polypeptide, whereas in the case of LHCII-neolute 2 luteins and 1 neoxanthin are coordinated to the complex.

Femtosecond transient absorption measurements were performed using a titanium-sapphire laser system. An oscillator (Tsunami, Spectra Physics, Mountain View, California) pumped by an argon-ion laser (Beamlok 2060, Spectra Physics), generated transform-limited pulses with a full-width-at-half-maximum (FWHM) of ~40 fs. These pulses were regeneratively amplified to 0.4–0.5 mJ, maintaining a pulse width of 70–80 fs (FWHM)

by chirped pulse amplification using a stretcher/compressor unit (model 4822, Quantronix, East Setauket, New York) and a regenerative amplifier (model 4810, Quantronix). The amplifier was pumped by a Q-switched Nd:YLF laser running at the second harmonic wavelength, 527 nm (model 527 DP-H, Quantronix). The pulse repetition rate of the amplifier was 3 kHz. A minor part of the amplified pulse was split off to generate a white light continuum for the probe pulse (~80 fs FWHM), while the major part was used to pump a traveling wave optical parametric amplifier (OPA) (Topas, Light Conversion, Vilnius, Lithuania). The OPA stage converted the wavelength to ~490 nm and ~500 nm with a pulse width of ~70 fs and a spectral width of ~4 nm. A pulse energy of ~1 nJ in a 120–130-μm diameter spot was used. A home-built camera system was applied to detect the absorption changes on ~250 wavelength channels simultaneously. The system is able to measure 3000 spectra/s from the diode array at full resolution of ~0.5 nm per pixel. Thus the camera covers a wavelength range of ~125 nm. The measurements were performed at 4°C in a vertically and horizontally shifted quartz cuvette with a pathlength of 1 mm with magic angle polarization between the excitation and probe pulses. Very low intensity of excitation was used to avoid annihilation effects. This was checked in a preliminary series of measurements by varying the excitation energy over a large range. Note that we are measuring LHCII monomers in this study. Thus the annihilation threshold is significantly higher than with LHCII trimers used in most previous studies. Furthermore, we used the lowest excitation intensities of all femtosecond measurements on LHCII reported so far. This can be judged from the final bleaching in the Chl a range after a few hundred picoseconds, which is only 0.5% of the maximal absorption in our case. The samples were measured at OD ~6–7 in the presence of 10 mM Hepes, pH 7.6, 0.06% DM, and an oxygen scavenging system (glucoseoxidase, catalase, glucose) (McTavish et al., 1989) to avoid photobleaching. The absorption and fluorescence spectra of the samples were measured before and after the femtosecond lifetime measurements, showing no changes due to photochemical or other damage.

Data analysis

The chirp in the white light continuum of ~4 fs/nm was corrected for in the data analysis. The visible and the blue/UV wavelength ranges have been analyzed separately. For each wavelength range two hypersurfaces describing a short 5-ps time range with 13-fs resolution and a long 300-ps range with 800-fs resolution have been measured and were analyzed simultaneously in the data analysis to cover both a long time range and high temporal resolution. The spectral resolution of originally 0.5 nm in the raw data files has been limited to 3 nm in any data analysis by binning several camera pixels, which results in a higher signal-to-noise ratio.

In general, the data were analyzed in two ways, first by the conventional global analysis in terms of a small number of discrete exponentials. It turned out, however, that the data contained too large a number of kinetic components that could not be resolved properly at most wavelengths, which led to sometimes severe deviations between fitted data and experiment. Thus these results were difficult to interpret and for this reason we do not present any results of this analysis here. Rather, we resorted to a lifetime distribution analysis method that was recently developed in our laboratory. The latter, the so-called lifetime density method, determines the pre-exponential amplitudes a_i in a sum of a large number (typically 70–100) of exponential functions with fixed lifetimes for each probe wavelength independently. The lifetimes τ_i in our case ranged from 13 fs to ~4 ns and were equally spaced on a logarithmic scale differing by a factor of 1.2.

The method is in principle similar to the ESM method introduced some time ago for the description of lifetime distributions (Siemiarczuk et al., 1990; James and Ware, 1986) but combines this method with a so-called regularization procedure as previously proposed by Kaufmann and coworkers (Landl et al., 1991). The well-known "maximum entropy method" (Brochon, 1994; Siemiarczuk et al., 1990; Ulrych and Clayton, 1976) presents just a special realization of a regularization procedure. The difference to the procedures described by Landl et al. and our method is the solution of the set of equations by a modified inverse Laplace transform, which reduces computation time and has the further advantage of being independent of starting values. The ESM method, without any further measures, would in addition to describing the underlying amplitude function, also try to describe the noise present in the data by an additional amplitude function that oscillates wildly. Thus the ESM method alone yields a minimal χ^2 value, i.e., an optimal solution in a purely mathematical sense. However, for practical purposes, analyzing real data with noise such a solution is usually not suitable due to the oscillatory part of the solution. The use of the regularization procedure ensures that the solution does not oscillate in the preexponential amplitudes of close-lying exponentials. Thus the effect of noise in the data, which causes these oscillations when no additional measures are taken, is avoided by the application of the regularization function. As a result, the algorithm in effect searches for a solution that still describes the data optimally, but filters out the noise at the expense of a slightly higher χ^2 value than the minimal one obtainable without regularization. The optimal set of parameters for the regularization function must be found for each problem at hand, the noise characteristics in the signal, etc. In general, the algorithm is allowed to increase the χ^2 values by up to 5–10% with respect to the estimated minimal possible value. Our method thus effectively combines the advantages of the ESM method and of the maximum entropy method. We have previously applied such a procedure to the analysis of photon echo data (Prokhorenko et al., 2000) (see there for further details and a more exact description of the method). Furthermore, the autocorrelation function P(Φ) required for deconvolution and the chirp of the white light continuum (taken into account as a wavelength-dependent shift Φ) was included in the algorithm.

Hence the model function to describe the transient absorption data $\Delta A(t, \lambda)$ for a certain detection wavelength λ_j looks as follows:

$$\Delta A(t, \lambda_j) = \int_0^t P(\phi) \cdot \left(\sum_{i=1}^{N} a(\tau_i, \lambda_j) \cdot \exp\left(-\frac{(t-\phi)}{\tau_i} \right) \right) d\phi \quad (1)$$

where N is a large number of typically 70–100 in the range from ~10 fs to 5 ns.

The procedure is applied independently to each wavelength channel of the data surfaces, i.e., no correlation has been assumed between nearby wavelength channels. The result is a three-dimensional density map $a(\tau_i, \lambda_j)$ for the probability of the presence of lifetime τ_i at wavelength λ_j (for this reason we call these plots "lifetime density maps"). Thus, in general, the lifetime components present in a signal can simply be depicted from this three-dimensional map. The absolute amplitude of a lifetime component is given by the integral over the node width along the direction of the lifetime axis. Several examples of lifetime density analyses on simulated data and their response to various levels of noise are given in the Appendix in order to get a better understanding of the properties of this method. The advantage of the method is that very complex kinetics with large numbers of exponentials can be still handled, which is not the case with other lifetime analysis methods. For discrete kinetics very close-lying exponential lifetimes can still be resolved, as is shown in the Appendix as well. Note that the width of a band in the lifetime space does not necessarily imply a distribution of lifetimes, but it is also controlled by the signal/noise ratio of the data (see Appendix).

RESULTS

In order to study the energy transfer process from carotenoids to Chls in LHCII complexes, we used reconstituted monomeric complexes in which we can vary the carotenoid composition. It has recently been shown that in LHCII there

are three carotenoids tightly bound to the complex. Two of them have been resolved in the LHCII structure and are located in the center of the complex forming a cross-brace between helices A and B. These two sites have a high affinity for lutein (Croce et al., 1999b; Hobe et al., 2000). A third carotenoid binding site has been recently located near the C helix domain (Croce et al., 1999a). This site accommodates only neoxanthin. In order to be able to discriminate between the transfer from the different carotenoids, two samples were used in the measurements. The Lhcb1 gene was expressed in *E. coli* and the reconstitution procedure was performed. In one case the pigment mix contained both lutein and neoxanthin (resulting in a sample called LHCII-neolutein henceforth), whereas for the second sample a pigment mix with only lutein as carotenoid was used (resulting in a sample called LHCII-lutein henceforth). The former one is very similar to w.t. LHCII containing three carotenoids, but in a more uniform fashion than the w.t. complex. The biochemical and steady-state spectroscopic characteristics of these two complexes have already been reported (Croce et al., 1999a, b). The Chl composition of the two samples is the same, and from the biochemical point of view the only difference is a neoxanthin molecule, which is lacking in the lutein only sample. It has been pointed out that this difference induces some small but significant spectral changes in a few of the Chls coordinated to the complex. In particular the absorption at 652 nm, typical for Chl b binding in the w.t. LHCII, is somewhat changed when neoxanthin is not present, indicating that this feature probably derives from some Chl-neoxanthin exciton interaction (Croce et al., 1999b).

The detailed transient absorption kinetics has been measured over two wavelength intervals (450–570 nm and 610–730 nm) for two excitation wavelengths in the carotenoid absorption region. The two wavelength intervals cover the transient absorption signals in the carotenoid S_2 absorption region and the Q_x/Q_y absorption regions, respectively. A very low excitation intensity has been used (<0.5% of the absorption of 0.7/mm at the absorption maximum of 675 nm of the Chls has been bleached at long times (300 ps after excitation)). The excitation intensity has been adjusted such that approximately similar excitation probability was achieved independent of the excitation wavelength. All measurements have been performed in the same way for the LHCII-neolutein and the LHCII-lutein samples. Fig. 1, *A* and *B* show some selected decay kinetic traces for the LHCII-lutein and the LHCII-neolutein samples, respectively.

For LHCII-lutein the decay in the Soret region for 500 nm excitation is faster than for the 490 nm excitation (Fig.

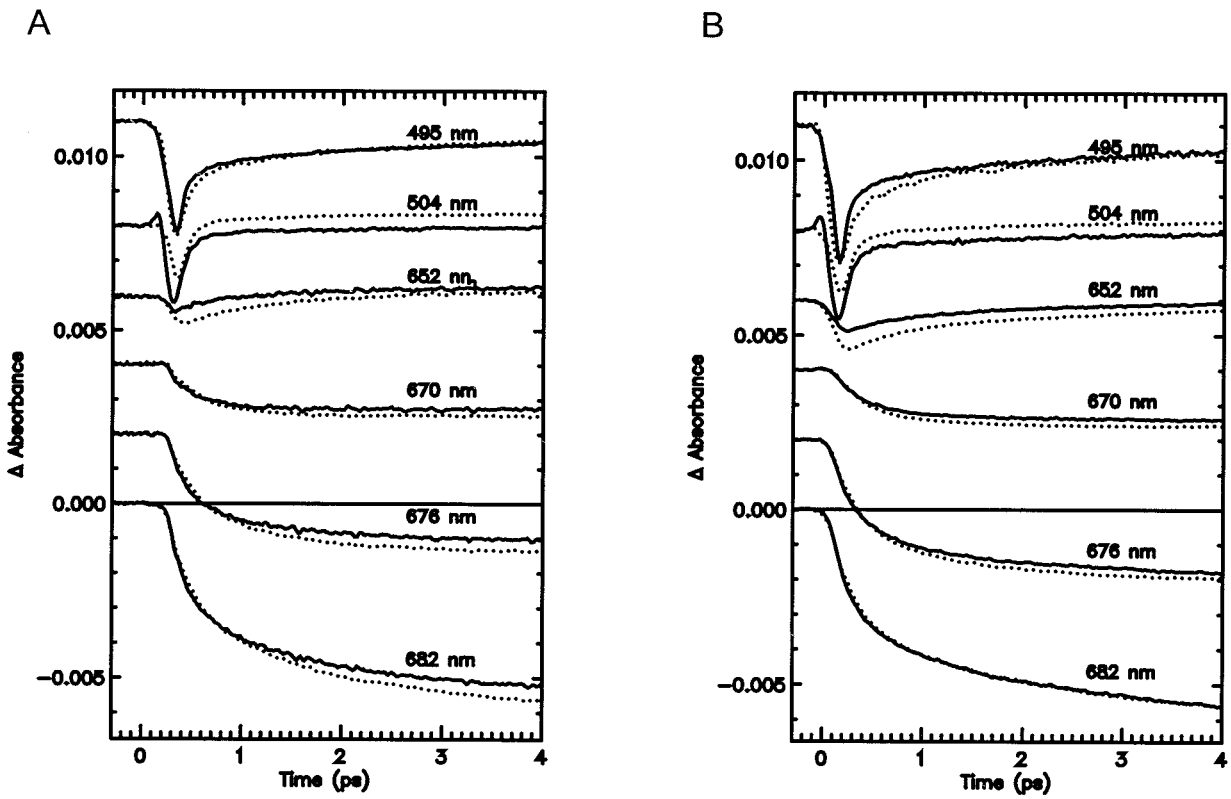

FIGURE 1 Experimental transient absorption kinetics for selected excitation/detection wavelength pairs for LHCII-lutein (*A*) and LHCII-neolutein (*B*). *Solid line:* excitation at 500 nm; *dotted line:* excitation at 490 nm.

1 *A*). In the Chl b region very rapid bleaching rise terms are observed with lifetimes below 100 fs, corresponding in their kinetics closely to the decay in the lutein absorption region. The amplitude of the rise term is more pronounced for 490 nm excitation. This points to a relatively small contribution by direct Chl b absorption, even for 490 nm excitation. In order to quantitatively account for the amount of Chl b absorption from an independent method, the Soret region of the absorption spectrum for both samples was reconstituted using the spectra of the single pigments (Croce et al., 2000) shifted to the red appropriately on the basis of results from previous experiments (Croce et al., 1999b). The spectrum of Chl b used in the fit has been obtained by analyzing two different LHCII samples with 7 Chl a and 5 or 4 Chl b. The difference spectrum obtained represents the absorption spectrum of Chl b in protein and shows a similar shape with respect to the spectrum in organic solvent, but the band is narrowed, as expected, by the effect of the protein environment. For the carotenoids the spectra in acetone were used, in accord with previous observations, which indicate that the spectrum of the carotenoids in proteins is identical in shape to their spectra in acetone (Croce et al., 2000). The fits of the Soret region of the absorption spectra for the two complexes are reported in Fig. 2, *A* and *B*. For both samples two Chl a forms, three Chl b forms and two lutein forms are used in order to obtain the best fit, and one additional neoxanthin form has been used for the LHCII-neolute in complex. The percentage of excitation in each pigment at the two wavelengths used in the experiments (490 nm and 500 nm) was calculated on the basis of the reconstituted absorption spectra, taking into account the width of the femtosecond excitation pulse. The data are reported in Table 1 for both samples. The data show furthermore that direct excitation of Chl b at 500 nm is essentially negligible. The best fits for both samples indicate that the two central luteins absorb at different energy, probably due to the protein environment in the L1 and L2 sites. This makes the excitation at 500 nm more selective for the "red" lutein.

For the LHCII-neolutein sample the carotenoid decay (almost exclusively lutein in this case) for 500 nm excitation (Fig. 1 *B*) is faster than for 490 nm excitation. Again, rapid rise terms of the bleaching in the Chl b region are observed, corresponding closely to the rapid decays in the Soret region. The bleaching rise terms are very pronounced for both excitation wavelengths. In comparison to the LHCII-lutein sample, a specific bleaching rise component due to neoxanthin can now be observed.

Fig. 3, *A–D* give the complete lifetime density maps in the Chl absorption region for the two excitation wavelengths and both samples. In Fig. 4, *A–D* the transient difference spectra at various selected delay times are given for the same data as shown in Fig. 3, *A–D*. These transient spectra were obtained from the corresponding lifetime density maps, i.e., they have been corrected for chirp in the laser pulses, and they have been deconvoluted with the excitation pulse.

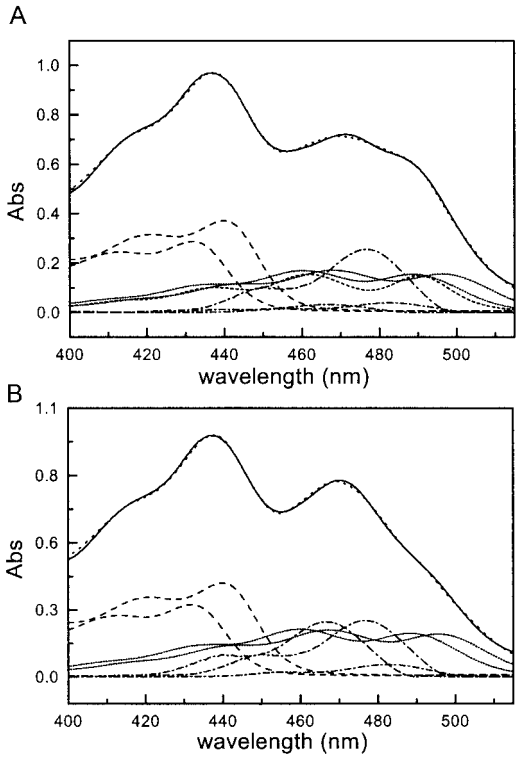

FIGURE 2 Description of the Soret region of the absorption spectra of LHCII-neolute in (*A*) and LHCII-lute in (*B*) in terms of the absorption of single pigments. The absorption spectra of both complexes (*solid line*) are compared with the reconstituted spectra obtained as a sum of the bands of the single pigments (*dotted line*). The spectra of the individual pigments are also shown: Chls a (*dashed line*), Chl b (*dot-dash*), lutein (*short dot*), neoxanthin (*short dash*).

For the LHCII-lutein sample (Fig. 3, *A* and *B*) a very pronounced bleaching rise term is observed in the 640–660 nm Chl b absorption region for 490 nm excitation. This rise time is in the range of 60–80 fs. For 500 nm excitation the amplitude of the bleaching rise term is weaker and the spectrum shows two maxima at 650 and 660 nm. The kinetics of this rise is in the ~50 fs range. At longer wavelengths (above 690 nm) under both conditions one sees a pronounced rise term in the excited state absorption (the

TABLE 1 Percentage of direct excitation of pigments in the Soret bands of the complexes on the basis of the fits shown in Fig. 2, *a* and *b*

	LHCII-neolute		LHCII-lutein	
	Ex 490 nm	Ex 500 nm	Ex 490 nm	Ex 500 nm
Chl a	2.4	4.1	2.9	5.0
Chl b	23.0	5.7	28.5	7.0
Lutein "blue"	25.8	28.0	34.9	36.7
Lutein "red"	25.2	39.8	33.7	51.3
Neoxanthin	23.5	22.5	–	–

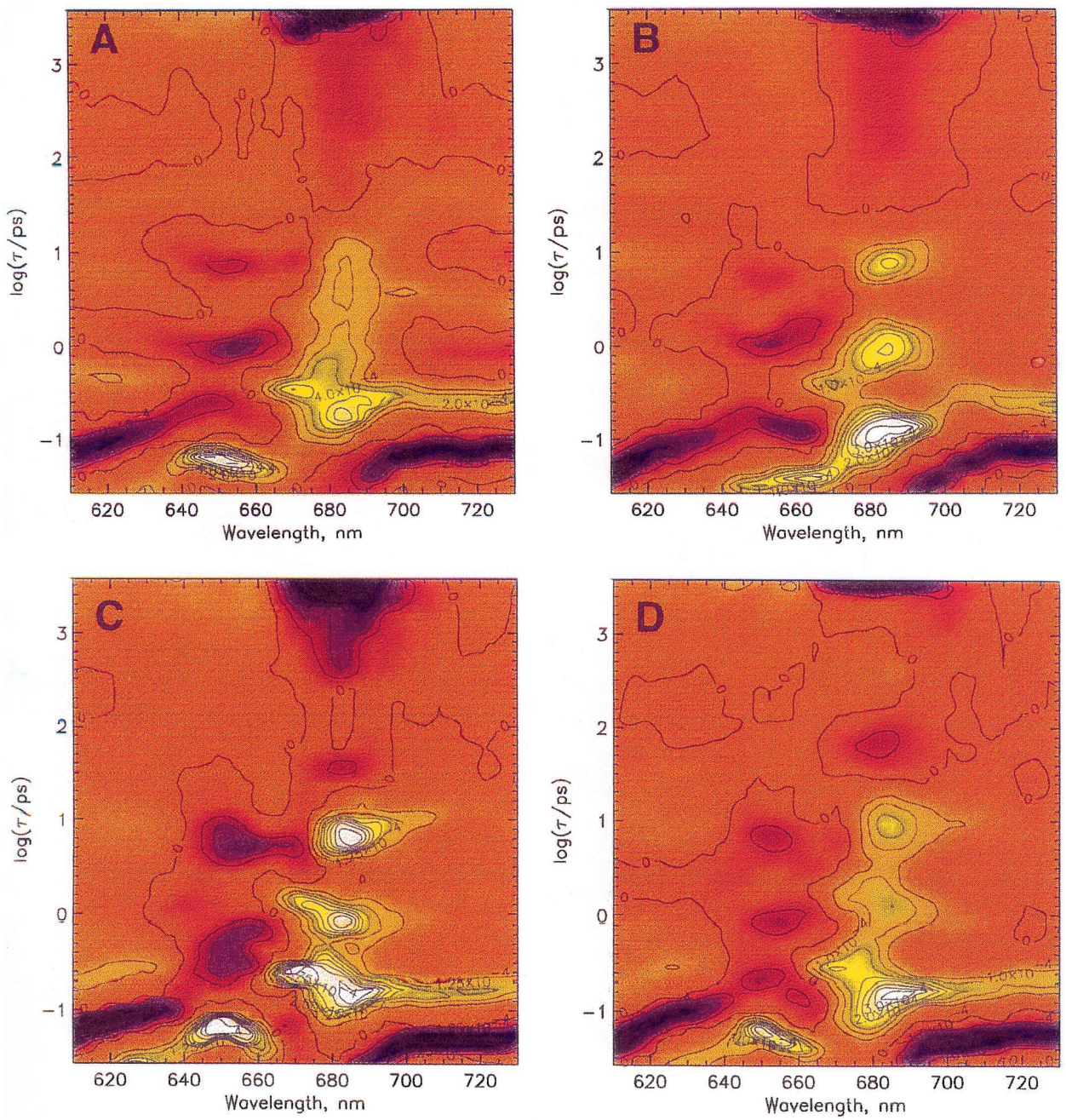

FIGURE 3 Lifetime density maps for LHCII-lutein (*top*) and LHCII-neolutein (*bottom*) for the two different excitation wavelengths of 490 nm (*left*) and 500 nm (*right*). *Note:* the red background denotes the zero level. Positive amplitudes are shown in yellow/white, and negative amplitudes are shown in blue/black (see Eq. 1). It is important to note that in transient absorption spectra a positive amplitude in a DAS can mean either a decay of excited state absorption or a rise in a bleaching signal. Likewise, a negative amplitude can either be a decay of the bleaching or the rise of an excited state absorption signal. Which possibility applies must be decided upon analysis of the lifetime density map and the whole kinetics. The lifetime scale shown is a logarithmic scale. It is important to note that these color maps represent a qualitative or at best semi-quantitative picture of the kinetics in a very condensed form. The density of the color has been chosen proportional to the amplitude, but due to printer and reproduction quality limitations one should be careful in the quantitative interpretation of the amplitudes based on these maps. Any quantitative information should only be deduced from the actual numerical amplitude distribution function underlying this surface (as, e.g., done here).

negative amplitude in that range cannot be due to a bleaching decay), which rises with the same kinetics as the bleaching in the Chl b region. This feature therefore should be mainly attributed to Chl b excited state absorption and in a somewhat smaller part to Chl a excited state absorption. Because neither Chl a nor Chl b alone when measured in

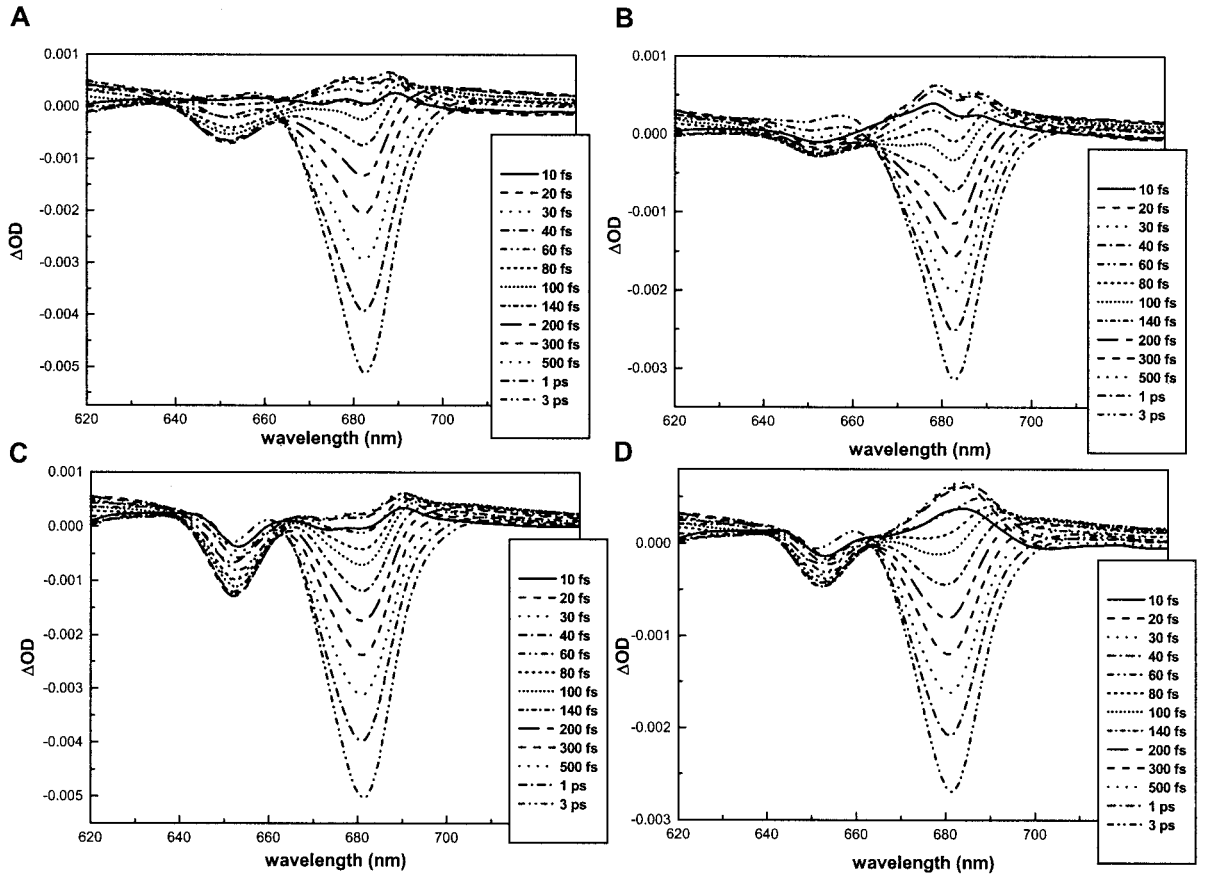

FIGURE 4 Transient difference spectra taken from the lifetime density maps in Fig. 3 for various delay times. The arrangement for samples and excitation wavelengths is the same as in Fig. 3.

solvents or when LHCII is excited in the Chl Q_y region directly shows such a strong excited state absorption signal in that range (data not shown), we attribute this signal to excited state absorption from higher states, i.e., starting from S_2 (Q_x) or S_3 (B_x) states. Although lutein also shows excited state absorption in that range when excited into the S_2 state, we can exclude that the observed excited state absorption rise is primarily due to carotenoids. The reason is that this excited state absorption feature decays mainly with a lifetime of ~300 fs (see complementary positive signal at that lifetime in Fig. 3, *A* and *B*) which is much slower than the carotenoid-to-Chl transfer, which seems to occur almost exclusively with lifetimes in the femtosecond range. The main processes of the Chl b-to-Chl a transfer occur with lifetimes of 170 fs, ~350 fs, ~1 ps, and ~10 ps (Fig. 3). It thus seems that the carotenoid-to-Chl transfer and the Chl b-to-Chl a transfers are quite well-separated in the lifetime range, which should make the detailed analysis somewhat simpler.

For the LHCII-neolutein sample (Fig. 3, *C* and *D*) there appears a pronounced new rise component (positive amplitude) centered near 650 nm. This must be a delayed rise of the bleaching in Chl b, and since this pronounced feature is not observed in the lutein-only sample it should be attributed primarily to the neoxanthin-to-Chl b transfer. This kinetics is somewhat slower (~90 fs) than the lutein-to-Chl b transfers (see above). In addition to that strong bleaching rise term in the Chl b region all the other rise components in the Chl b region are seen as well as in the lutein-only sample. In addition to the ~1 ps and 10 ps decays in the Chl b region and the corresponding rise term of the bleaching in the Chl a region, which all were seen already in the lutein-only sample, a new Chl b-to-Chl a energy transfer time with a lifetime of ~300–400 fs shows up in the LHCII-neolutein sample. Table 2 summarizes the characteristic ranges of lifetimes observed in the lifetime density maps along with a qualitative assignment for the various excitation wavelengths.

Fig. 5 shows the transient absorption spectra for early delay times of the LHCII-lutein sample when excited into the Chl b absorption range at 640 nm. Only after ~50–70 fs is a "normal" Chl b bleaching spectrum near the excitation wavelength observed. These early features around the excitation wavelength are due to four-wave-mixing effects and will not be considered here. However, in the Chl a region unusual features are also observed around 680 nm. These

TABLE 2 Summary of observed lifetimes, wavelength ranges of observation, and assignments of components

Lifetime	Wavelength Range of Observation	Assignment
50 fs	490–500 nm; 640–655 nm	Lutein 2 to Chl transfer
70 fs	490–500 nm; 640–655 nm	Lutein 1 to Chl transfer
90 fs	490–500 nm; 640–655 nm	Neoxanthin to Chl transfer
170 fs	640–655 nm; 660–685 nm	Chl b to Chl a transfer
200–300 fs	above 690 nm	Chl b Q_x state relaxation
330 fs	640–655 nm; 660–685 nm	Chl b to Chl a transfer
900 fs	525–560 nm	Unassigned; possibly vibrational relaxation in S_1 state of a carotenoid
1 ps	640–655 nm; 660–685 nm	Chl b to Chl a transfer
7 ps	640–655 nm; 660–685 nm	Slow Chl b to Chl a transfer
3.9 ps	525–560 nm	Lutein S_1 relaxation
14.5 ps	525–560 nm	Lutein S_1 relaxation
Several ns	670–690 nm	Overall Chl a excited state decays

are far away from the excitation wavelength and cannot be explained primarily by four-wave-mixing effects. Rather, the pronounced absorption increase at early times must be attributed to Chl b/Chl a exciton coupling (Valkunas et al., 1999). Quite similar effects were also observed with the LHCII-neolutein sample (data not shown). The excited state absorption decays within ~50–70 fs, i.e., within a time when no substantial amount of Chl b-to-Chl a energy transfer has occurred. Apparently some excited state dynamics in the Chl b/a excitonically coupled pairs occurs upon Chl b excitation, which leads to a strong excited state absorption and thus to a distortion in the kinetics in the Chl a region. One can also exclude these distinct spectral features located in the Chl a absorption region to be simply due to Chl b excited state absorption. Chl b, when measured in solution (data not shown), shows a small but spectrally flat excited state absorption signal in the long-wavelength region. This effect will be crucial to take into account when analyzing the carotenoid-Chl energy transfer data, because such excited state features appear in those data with the same kinetics as when the carotenoid-Chl b transfer occurs; i.e., while the excited state absorption appears promptly when Chl b in LHCII is excited directly, the excited state absorption feature appears with the rise time of the carotenoid-Chl b energy transfer (see Figs. 3 and 4) when carotenoids are excited. The most pronounced rise can be seen for the LHCII-neolutein sample for excitation at 500 nm (Fig. 4 *D*), but it is present under all the conditions measured here.

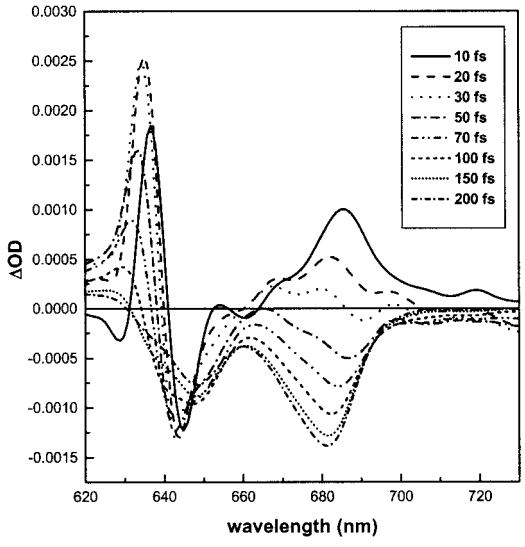

FIGURE 5 Transient absorption spectra for early delay times of the LHCII-lutein sample upon excitation into the Chl b absorption region at 640 nm.

DISCUSSION

The comparison of the data obtained from two different samples, differing in their carotenoid content and with different excitation wavelengths, allows drawing some very detailed conclusions about the principal features of the carotenoid-to-Chl transfer. In the following we will develop a detailed qualitative model for these transfer steps on the basis of these data, and also discuss some peculiarities in the spectra that complicate the development of a quantitative model. We will address and discuss in particular the following points:

1. All carotenoid-to-Chl transfer starting from the S_2 state of carotenoids occurs with time constants below 100 fs;
2. Chl b-to-Chl a transfer is well-separated in time from the carotenoid-to-Chl b transfer (the fastest Chl b-to-Chl a transfer time is ~150 fs);
3. A large part (~50%) of the initial carotenoid excitation is transferred via Chl b to Chl a, and three different Chl b molecules receiving energy directly from carotenoids can be distinguished;
4. The two luteins can be distinguished spectrally and in their kinetics and energy transfer pathways;
5. Specific coupling effects between Chl b and Chl a excited states previously led to some underestimation of the direct carotenoid-to-Chl a transfer;
6. The dominant part of the carotenoid-to-Chl transfer occurs from the S_2 state of the carotenoids;
7. The carotenoid-to-Chl transfer, in particular to Chl b, occurs via both the Q_x and the B_x states, which leads to a further complication in the analysis;
8. We find no evidence for substantial S_1 carotenoid-to-Chl transfer but cannot entirely exclude such a pathway for the neoxanthin molecule.

Carotenoid-to-Chl b transfer

For both samples under all excitation conditions fast bleaching rise times in the range of 50–90 fs occur in the Chl b

absorption regions. The maxima of the bleaching bands appear in two different spectral ranges at 645 nm and at 655–660 nm (cf. the positive amplitudes in that range in Fig. 3, *A–D*). The bleaching rise term around 660 nm is always faster than the rise at 645 nm. The fastest bleaching rise term with ~50 fs lifetime occurs for the LHCII-lutein samples with 500 nm excitation, while the slowest one (~90 fs lifetime) is observed in the LHCII-neolutein sample for both 490 and 500 nm excitation. In all spectra (Fig. 3) a broad negative feature with the same lifetime as the delayed rise in Chl b bleaching and the bleaching decay of the carotenoids, i.e., with lifetimes shorter than 100 fs (Fig. 4) occurs in the wavelength range above 690 nm. This broad negative amplitude feature cannot be the decay of an absorption bleaching that occurs due to direct excitation of an excited state by the laser pulse because there is no ground state absorption in that wavelength range. It can thus only be interpreted as the delayed rise of an excited state absorption. In that case it must be due to Chl b excited state absorption, which represents second independent evidence in favor of an efficient direct carotenoid-to-Chl b transfer. This broad spectral feature decays on the time scale of 200–300 fs, depending on the sample and excitation conditions, with a kinetics that corresponds approximately to the rise time in Chl a bleaching. The comparison of the dominant component in the decay of the carotenoid bleaching and the rise in the Chl b and Chl a regions strongly suggests that the overwhelming part of the energy transfer occurs from carotenoids in their S_2 state to the Chls, and only a minor part might pass the S_1 state of the carotenoids. The question of a possible minor S_1 pathway will be discussed below.

Chl b-to-Chl a transfer

From the data shown in Figs. 3 and 4 it is possible to assign four different transfer components from Chl b to Chl a. The fastest one is 170 fs, the second is 330 fs, a transfer in the 1-ps range and a slow one in ~7 ps. This means that with respect to previous measurements one additional transfer component is observed. The 600 fs observed previously by several groups (Connelly et al., 1997b; Trinkunas et al., 1997; Kleima et al., 1997; Visser et al., 1996) is not found in our present data but is replaced by two transfer components with 330 fs and 1 ps lifetime. The same components are also observed when the Chls b are directly excited (see, e.g., Fig. 5), which confirms that this new transfer time is indeed due to Chl b-to-Chl a energy transfer and is not influenced by the carotenoid-to-Chl transfer. The ~600 fs component resolved previously is thus likely to be a mixed component that arose from the 330 fs and 1 ps components. The LHCII complex analyzed here has 12 Chls with Chl a/b of 1.6. We thus expect in principle 5 Chl b-to-Chl a transfer components. However, not all of them will necessarily show up in the carotenoid-to-Chl transfer measurements. In our present data with carotenoid excitation the contribution of the 330 fs transfer is almost absent when the LHCII-lutein sample is excited in the carotenoid region, whereas it is quite pronounced for the LHCII-neolutein sample. This is an indication that the one or two Chl b molecules that transfer to Chl a with a 330 fs lifetime are located near the neoxanthin molecule. It is thus possible to suggest that the Chls in sites B5 or B6 (using the Kühlbrandt nomenclature (Kühlbrandt, 1994)) are involved in this transfer involving Chls b absorbing around 652 nm, exactly the wavelength at which the Chls in sites B5 and B6 are expected to absorb on the basis of the mutation analysis (Remelli et al., 1999). We propose that the acceptor of this transfer is the Chl a in site A5, which absorbs at 675 nm according to the mutation analysis.

All pronounced rise time components that are observed in the Chl a bleaching range of 670–690 nm occur on a slower time scale than the rise of the Chl b bleachings or the decay of the carotenoid bleachings (Figs. 3 and 4), i.e., ~150 fs lifetimes. From the qualitative analysis performed here we cannot exclude a contribution of Chl b-to-Chl a energy transfer arising from a direct excitation of Chl b. In fact, the amount of direct Chl b excitation at these wavelengths has recently been a matter of debate (Connelly et al., 1997a; Peterman et al., 1997b). We have recently proposed a method for a detailed analysis of the absorption spectra of the LHC complexes in the carotenoid region (Croce et al., 2000). This analysis allows for an exact calculation of the absorption contributions of Chl b and carotenoids in the LHCII complexes and it has been applied here to both samples. As reported in Table 1, the Chl b excitation for 500 nm pulse excitation in our experiment is negligible, whereas for 490 nm excitation the maximum relative contribution is ~25%. For all practical purposes of this qualitative analysis we can ignore this small percentage of direct Chl b excitation at 500 nm. This means that no substantial part of the Chl b-to-Chl a transfers seen in Fig. 3 is due to direct Chl b excitation, but rather arises from the ultrafast carotenoid-to-Chl b transfer, as detailed above. Thus we cannot reconcile the fast rise in the Chl b bleaching with any other process than carotenoid-to-Chl b transfer.

Direct carotenoid-to-Chl a transfer

In all spectra in Fig. 3 some part of the bleaching rise in the Chl a absorption range occurs with the same lifetime as the Chl b bleaching rise, and in particular the rise of the excited state absorption above 690 nm. In the range of 680–690 nm this strong excited state absorption partly compensates the opposite amplitude bleaching signal in Chls a. These observations clearly indicate that a substantial part of the carotenoid excitation is also transferred directly to Chl a. The rise in the Chl a bleaching in general seems to be slightly slower as compared to the carotenoid bleaching decay and Chl b bleaching rise. This slight delay probably indicates some more complex photophysics (see below for a further dis-

cussion). When examining the difference spectra at various delay times (Fig. 4) the direct carotenoid-to-Chl a transfer is not obvious at first glance because a bleaching in the Chl a Q_y absorption range occurs only at times above ~140 fs, while at earlier times an excited state absorption is observed. This rise in excited state absorption is quite pronounced in some cases (see e.g., Fig. 3, *A* and *B*) with an absorption at 680–685 nm that exceeds the bleaching in the Chl b absorption range. The reason for this bleaching must be a pronounced Chl b-Chl a coupling, presumably due to excitonically coupled pairs. This coupling is seen also in the transient spectra upon direct excitation of Chl b (cf. Fig. 5). However, in that case the absorption increase in the Chl a region appears promptly with the excitation pulse, while in the carotenoid excitation case (Fig. 3) it rises with a rise time of the carotenoid bleaching decay. We have previously described this phenomenon as arising due to exciton coupling, and it can be described theoretically when dropping the Heitler-London approximation (Valkunas et al., 1999). These findings have important consequences for the interpretation of the carotenoid-to-Chl transfer in LHCII. First, this observation provides a third independent evidence for a major direct carotenoid-to-Chl b transfer pathway. Furthermore, the absorption increase in the Chl a region compensates the initial Chl a bleaching due to direct carotenoid-to-Chl a transfer. Only after ~100 fs the signal in the Chl a absorption range turns into an overall bleaching signal. This feature thus hides the effects of an early carotenoid-to-Chl a transfer and was responsible inter alia for an underestimation of the direct carotenoid-to-Chl a transfer contribution in our earlier study on LHCII (Connelly et al., 1997a). It can be clearly seen from Fig. 4 that only after ~150 fs, at a time when the Chl b bleaching signal is still at its maximum, a distinct Chl a bleaching has developed due to the decay, probably by dephasing of the exciton states, of the Chl a absorption increase. Any quantitative kinetic model thus should use only the signal from ~150 fs onward to describe the development of concentration ratios of excited Chl b/Chl a due to the carotenoid Chl b-Chl a transfer kinetics. Due to the very fast Chl b/Chl a transfer (main components of 170 and 330 fs) following the carotenoid-to-Chl b transfer, the Chl b bleaching maximum at any time is much smaller than the total amount of carotenoid-to-Chl b transfer. A crude kinetic model based on these transfer lifetimes and taking into account the bleachings observed in the Chl b and Chl a ground states at early and late times, respectively, indicates that ~40% of the energy transferred from carotenoids takes the Chl b pathway. Peterman et al. (1997b) reported that in LHCII the carotenoids transfer only to Chl a with a lifetime of 200 fs. This discrepancy with our data can be due to the insufficient temporal resolution in their measurements that did not allow proper resolution of the ultrafast carotenoid-to-Chl transfer, which is faster than 100 fs. In this case the first part of the energy transfer pathway from carotenoids to Chl b would be missing in their data, and only the second part involving the transfer from Chl b to Chl a would have been resolved.

Two different luteins

Some distinct differences occur in the delayed rise of the Chl b bleaching in the LHCII-lutein sample: upon excitation at 500 nm the overall rise in Chl b bleaching occurs faster (more close to 50–60 fs) and the bleaching maxima are located at longer wavelengths (650 nm and 665 nm as compared to 645 nm and 650 nm) than for excitation at 490 nm. This is a consequence of the slightly different absorption maxima of the two luteins in LHCII that has been found in our absorption analysis. We can thus conclude that the two luteins transfer their energy to at least two different Chl b molecules that have bleaching maxima at 645 nm and 650–655 nm. One or two further Chls b receive energy from the neoxanthin, which can be seen clearly by comparing the lifetime density plots (Fig. 3) and the transient spectra (Fig. 4) for the two different samples. Overall, the transfer from neoxanthin to Chls is significantly slower, i.e., more close to 90 fs lifetime, as compared to the lutein transfer.

Transfer via the S_1 level of carotenoids

To understand if and how much energy might be flowing via the carotenoid S_1 state after excitation in the S_2 state the results of pump-probe experiments on lutein in diethylether (data not shown here) and of LHCII, which contains only lutein as carotenoids, have been compared. The ratio between the area of the S_1-S_n excited state absorption of the carotenoids (when at maximum) and the area of the bleaching in the carotenoid S_2 band immediately after excitation in the S_0-S_2 transition have been compared for these two samples considering the maximal amplitudes of the bleaching and the maximal amplitude in the S_1-S_n carotenoid excited state. This ratio is 11.5 in the case of lutein in organic solvent, whereas it is reduced at 2.2 in the case of the LHCII complex. From that we can estimate that not >20% of the energy absorbed in the S_2 state can flow into the S_1 state of the carotenoids when lutein is bound to LHCII. The analysis of the transient profiles associated with the build-up and the decay of the spectral features in the 535–555 nm region show that there is a rise time of ~50–100 fs for the excited state absorption and the decay can be described with three different lifetimes: of 3.9 ps, 15 ps, and 2.27 ns. Based on its spectrum and lifetime the last one is most probably associated with the presence in the same region of some S_1-S_n transition of Chl a. Due to the very intense S_1-S_n absorption of carotenoids we can detect the carotenoid S_1 state and its kinetics quite easily in transient absorption data in the 540 nm range, even when the relative population of this state is much less than 20%. The Chl

S_1-S_n ESA is at least 10 times less intense with respect to the one of carotenoids, and its presence is most pronounced at long times (above 50 ps) when all the carotenoid excited states have already decayed. The most pronounced lifetime in the S_1-S_n ESA of carotenoids of 15 ps is very similar to the S_1 lifetime of lutein in solution (14.6 ps; Frank et al., 1997), suggesting that at least one of the luteins does not transfer energy from the S_1 state (cf. Fig. 6). There does not seem to be a Chl transfer component in that range that could interfere with the assignment of that component. The second lutein ESA component has a decay time of 3.9 ps. The shorter lifetime of the second lutein could be due to energy transfer to Chls from the S_1 state or could be due to a faster radiationless relaxation, because the conformation might be different with respect to solution. The amplitude of this component is substantially lower than the amplitude of the 15 ps component and its spectrum peaks at 555 nm. The ratio of the amplitudes between the two components is higher when the sample is excited at 500 nm (data not shown). The rise time of 50–100 fs for the ESA in that range is in agreement with the $S_2 \rightarrow S_1$ transition of the lutein, which should rise with the S_2 decay time, which in turn is controlled by the direct S_2-to-Chl transfer rates. The agreement of the S_1 excited state absorption rise time with the rise time of the Chl b bleaching provides further support that the major energy transfer pathway is directly from the S_2 state of carotenoids. We conclude that ~70% of the energy absorbed by luteins is directly transferred to Chls via the S_2 state. Because this represents nearly the overall efficiency of the transfer of luteins to Chls in this complex, there is little room for a significant transfer pathway via the S_1 state.

We expect an S_1 lifetime of neoxanthin of ~35 ps when unquenched (Frank et al., 2000). In the LHCII-neolutein sample we do not find such a lifetime for decay of excited state absorption, however, suggesting that the S_1 decay is shorter than in solution, presumably due to some energy transfer to Chls. Thus neoxanthin might be the only candidate that could transfer to a significant amount via the S_1 state to the Chls. We do not observe a clear signal that we could attribute to such a process. One possibility is that the lifetime is similar to that of one of the luteins (i.e., ~15 or 3.9 ps) by accident. The small differences between the two samples in the respective lifetime range and wavelength region do not positively support such an interpretation. Another possibility would be to assign a small component of ~300 fs that is present in our data for the LHCII-neolutein sample. It seems, however, that this component is more likely due to Chl b-to-Chl a transfer because it is also observed in the LHCII-lutein sample. In a recent work from the Fleming group (Walla et al., 2000) two-photon excitation has been used to excite the carotenoids directly into the S_1 state and observe the energy transfer to the Chls. Surprisingly, a fast subpicosecond rise time in Chl fluorescence attributed to energy transfer from the S_1 state has been found. The work of Walla et al. did not specify which carotenoid did show the fast energy transfer to Chls upon two-photon excitation, however. Thus, in order to get an agreement with our data, one might attribute it to neoxanthin, but not to the luteins. A new problem arises, however, if the S_1 lifetime of neoxanthin should be as short as suggested by the data of Walla et al.: the subpicosecond lifetime of the S_1 state would imply that energy transfer from that state would be nearly 100%. This is difficult to

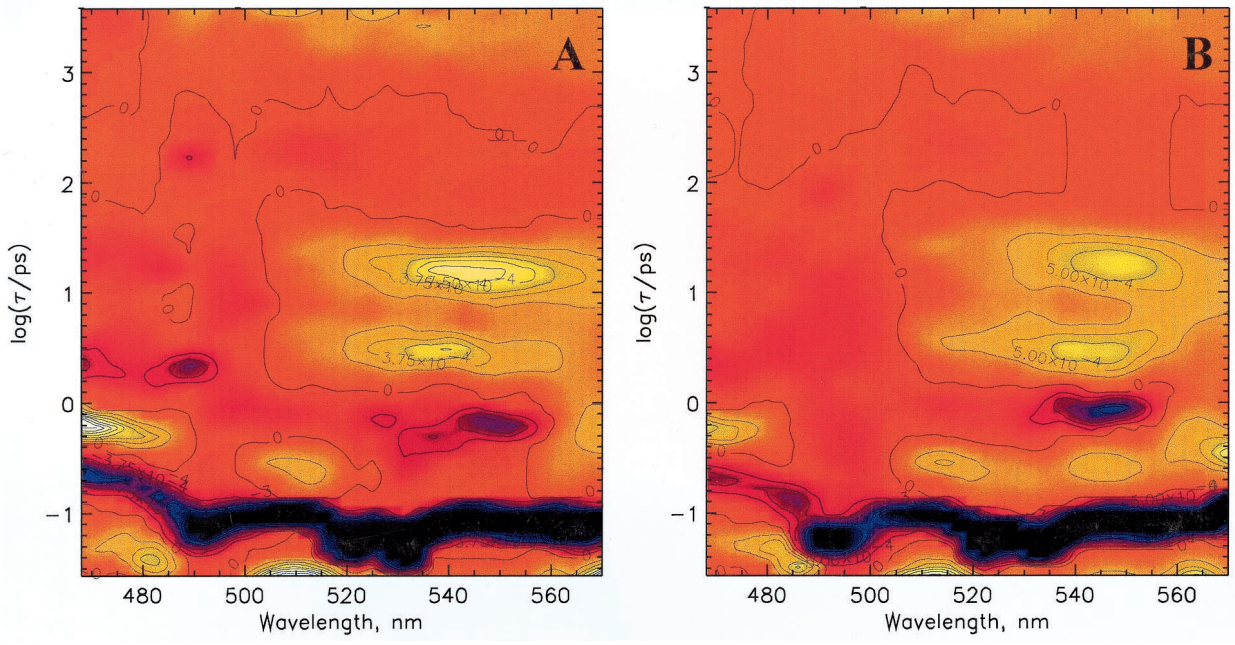

FIGURE 6 Lifetime density maps in the carotenoid absorption region. *Left:* LHCII-lutein; *right:* LHCII-neolutein. λ_{exc} = 490 nm. See Note, Fig. 3.

reconcile with our finding from steady-state fluorescence that the overall neoxanthin transfer efficiency is only ~50% (Croce, unpublished results), which is explained almost entirely by the S_2 transfer path already. Clearly, a more detailed analysis and investigation is required to clarify these discrepancies. We note, however, that Walla et al. (2000) also found in addition much slower (long ps) S_1 decay components (and corresponding Chl fluorescence rise times) which are well in line with our findings for the lutein S_1 decays in the picosecond range. Provided that a two-photon excitation of the Q_x-state of Chls can be excluded as a possible cause of the ultrafast Chl fluorescence lifetime (such a ~300 fs rise time could be due to internal conversion from the Q_x-state and subsequent vibrational relaxation) another possibility exists to explain the ultrashort rise time in the Chl fluorescence found by Walla et al.: after internal conversion to the carotenoid S_1 state the system is in highly excited vibrational states. As will be seen from our data on lutein in solvents (to be published) the vibrational relaxation is a multi-component process with lifetimes ranging from ~200 fs to nearly 1 ps. These high vibrational states while relaxing might have a much higher efficiency of energy transfer due to substantially better spectral overlap with the B_x state of Chl b than the vibrationally relaxed state, which indeed has a several picosecond lifetime. The rise time observed in the Chl fluorescence due to such an energy transfer would then not reflect the actual energy transfer time, but rather the vibrational relaxation time in the carotenoid S_1 state. Such an interpretation would appear to be in good agreement both with our present data and with the data of Walla et al. (2000).

Which Chl states are accepting energy?

The most likely energy transfer mechanism between carotenoids (in their S_2 state) and Chls is via the Förster mechanism. Even for carotenoid S_1 transfer paths Förster transfer might be more efficient than a Dexter mechanism (Damjanovic et al., 1999). However, the overlap integral for the S_2 fluorescence with the Chl Q_y absorption of both Chls b and a is quite small. This suggests that the energy-accepting state in the Chls is actually not the Q_y, but rather the Q_x state for Chl a and both the B_x and the Q_x states for Chl b. Results of Förster rate calculations strongly support this interpretation (see part II of this work for detailed calculations). A schematic presentation of the energy transfer paths taking into account all these findings is given in Fig. 7. Such a pathway provides a further complication for the quantitative modeling of the kinetic data of the carotenoid-to-Chl transfer. This will complicate the interpretation of both the Chl b bleaching rise and the Chl a bleaching rise. A first rise in Chl b and Chl a bleaching in their Q_y bands will occur with the carotenoid-to-Chl transfer time. However, if the accepting state is the Q_x state, a second rise component should

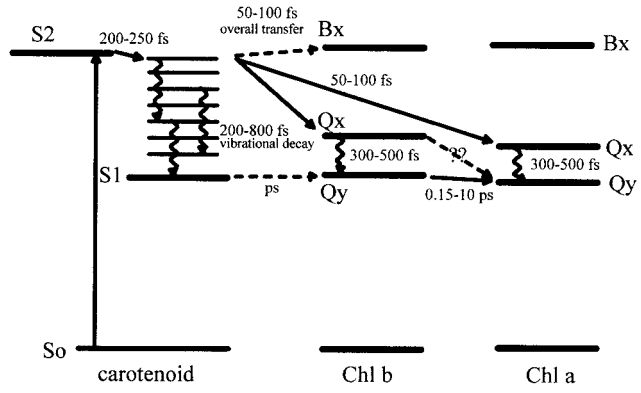

FIGURE 7 Qualitative kinetic scheme for energy transfer from carotenoids to chlorophylls in LHCII (cf. Fig. 8).

occur with the relaxation time from Q_x to Q_Y, i.e., in the ~200–500 fs range for the stimulated emission contribution to the formal bleaching signal. We do not observe such a second slower component in the rise of the Chl b bleaching, but we observe the decay of the strong excited state absorption signal of Chl b in the range above 690 nm. This decay occurs with ~300 fs lifetime and cannot be due to Chl b S_1 absorption, as indicated above. This is a strong indication that Chl b actually gets excited into either its Q_x or its B_x state, or both, by energy transfer from the carotenoids. The 300 fs decay of the S_2 excited state absorption might then reflect either direct energy transfer from the Chl b S_2 state to Chl a or a radiationless relaxation to the Q_y state. If the former was the case (actually both pathways may occur in parallel) it would be difficult to observe it in our data because there is a proper Chl b-to-Chl a transfer component in the same lifetime range, which can be observed upon direct Chl b excitation (Fig. 5 and data not shown). In any case, this mechanism will lead to a severe underestimation of the carotenoid-to-Chl b transfer efficiency if only measured from the amplitude of the Chl b bleaching because up to 50% of the signal in the Chl b bleaching region might actually be missing if the excited state initially produced is in fact the Q_x state. However, due to the same mechanism the rise in the Chl a bleaching due to direct energy transfer from the carotenoids might be delayed substantially if Chl a

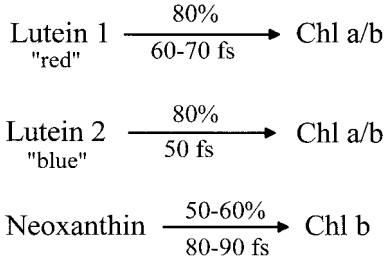

FIGURE 8 Schematic kinetic diagram of principal energy transfer pathways in LHCII.

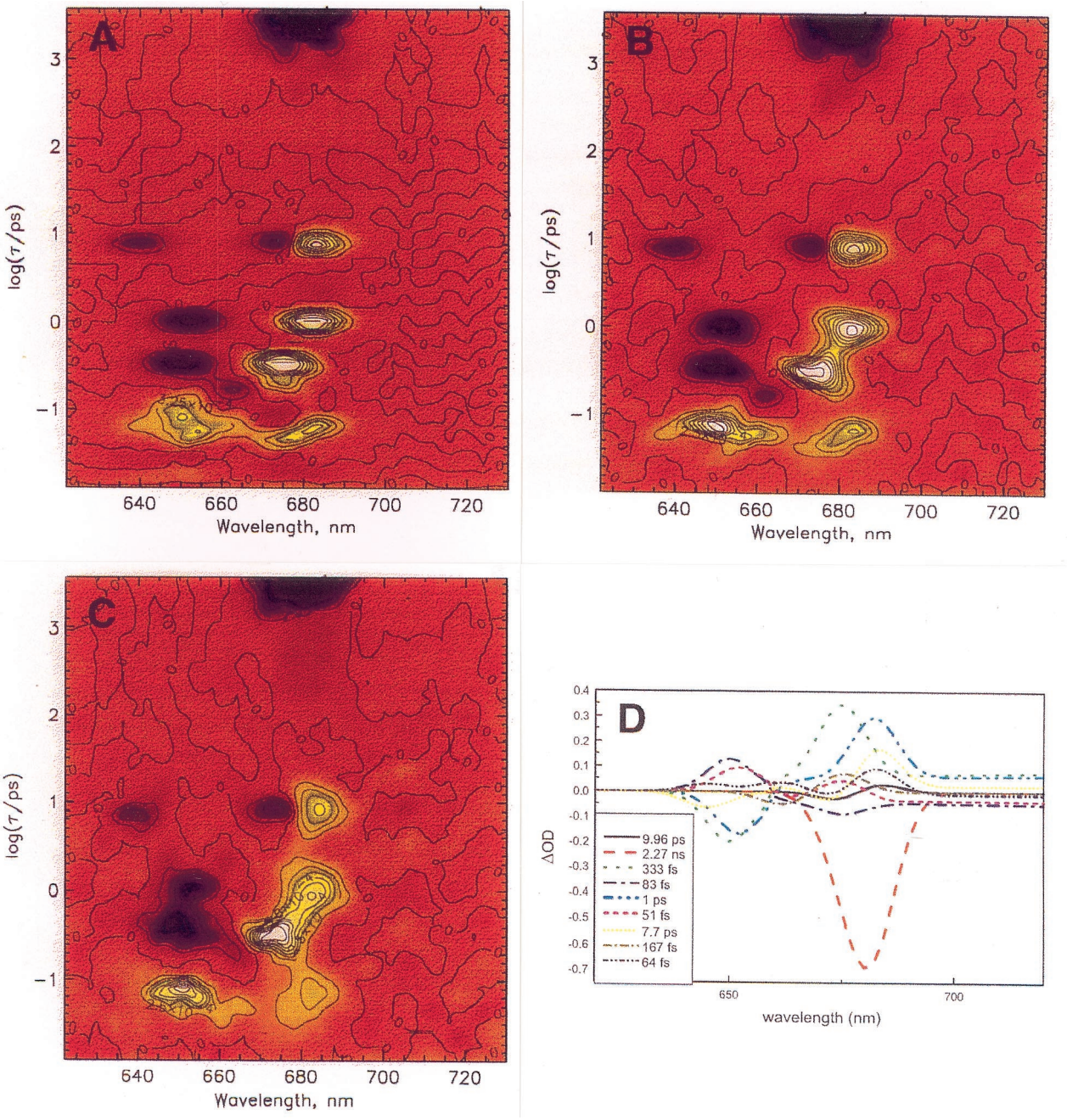

FIGURE 9 (*A–C*) Lifetime density maps calculated from simulated transient absorption data (cf. Fig. 9 *D*) with different noise levels added. (*A*) Very low noise level; (*B*) noise level typical for the transient absorption measurement presented in this work; (*C*) five times higher noise level than in (*B*). See Note, Fig. 3, for the representation. (*D*) Set of DADS used for simulating a data set that is similar in complexity as expected for the LHCII kinetics problem.

accepts energy from carotenoids into its Q_x state, which is highly likely. This will lead to a further complication in the quantitative analysis of the Chl a bleaching kinetics. Besides a somewhat lower time resolution and insufficient spectral information it was mainly these complex features that led us to underestimate the contribution of direct carotenoid-to-Chl a transfer somewhat in our previous work (Connelly et al., 1997a).

APPENDIX

In order to be able to better judge the capabilities of the lifetime density analysis we simulated a couple of data sets with a complexity similar to that expected for the LHCII system. To this end we set up a simplified kinetic scheme and intermediate spectra for different components similar to those expected for LHCII. Note that this should be considered strictly to represent a simulation to learn about the limits and capabilities of this method to separate a complex multi-exponential kinetics, and not as an

attempt to actually quantitatively model the LHCII data, which will be done separately. In principle we expect some 15 lifetime components from LHCII (12 for Chl-Chl transfer and 3 for carotenoids) in the simplest kinetic model. This is a highly complex kinetic data set that far exceeds the capabilities for analysis by more conventional methods. Note that we are simulating here only discrete kinetic models, which are probably the best description for the data at hand for LHCII. The lifetime density analysis is, however, equally suitable and very powerful for the analysis of both discrete and inherently dispersive kinetics.

Fig. 9 *D* shows one of the simulated sets of decay-associated absorption difference spectra (DADS) and lifetimes that define the simulated data surface. The kinetics at a number of wavelengths was then calculated from these data and random noise was added at various levels. The data in the form of a simulated $\Delta A/\lambda_{det}$/time surface were then subjected to the lifetime density analysis in the same way as experimental data. The results are shown in Fig. 9. Fig. 9 *A* shows the recovered map when only a minimal amount of noise, significantly smaller than achievable in an experiment, is added. In this case all lifetime components are quite well resolved. Even the ~50 fs and ~100 fs components in the 650 nm range and around 670–680 nm can be separated quite well. When more noise is added, as in Fig. 9 *B* where the noise level is characteristic of the noise level in a typical experiment, some of the previously better-resolved features start to blur. In that case close-lying lifetimes may not be fully resolved anymore; however, the center of the band can still be localized and lifetime differences can be seen relatively easily. In fact, in this case all the major lifetime components in this complex data set can be observed quite well. Again, the 50 fs and 100 fs components are still resolved reasonably well, although the different bands already start to smear out. When attempting to resolving this complex data set by the less sophisticated global lifetime analysis, let alone a single decay analysis, as often used for analyzing such data, we could not resolve more than 5 to 6 components. The resolved lifetimes generally were mixed ones that did not allow for a clear insight into the underlying spectra and kinetics. Thus the lifetime density maps provide a much superior picture of the kinetics to one that can be obtained using any other of the typically used kinetics analysis methods. Finally, the effect of an even higher noise level (5 times higher than in Fig. 9 *B*) is shown in Fig. 9 *C*, where many of the previously resolved features start to blur. This well demonstrates the effect of noise on the resolution (width of the bands in lifetime space) and the importance of a high signal/noise ratio in the data.

R.C. was supported by TMR Marie Curie Fellowship Grant ERBFM-BICT983216.

REFERENCES

Barzda, V., E. J. G. Peterman, R. van Grondelle, and H. Van Amerongen. 1998. The influence of aggregation on triplet formation in light- harvesting chlorophyll a/b pigment-protein complex II of green plants. *Biochemistry.* 37:546–551.

Bassi, R., R. Croce, D. Cugini, and D. Sandona. 1999. Mutational analysis of a higher plant antenna protein provides identification of chromophores bound into multiple sites. *Proc. Natl. Acad. Sci. U.S.A.* 96: 10056–10061.

Bassi, R., D. Sandona, and R. Croce. 1997. Novel aspects of chlorophyll a/b-binding proteins. *Physiol. Plant.* 100:769–779.

Bittner, T., K-D. Irrgang, G. Renger, and M. R. Wasielewski. 1994. Ultrafast excitation energy transfer and exciton-exciton annihilation processes in isolated light harvesting complexes of photosystem II (LHCII) from spinach. *J. Phys. Chem.* 98:11821–11826.

Bittner, T., G. P. Wiederrecht, K-D. Irrgang, G. Renger, and M. R. Wasielewski. 1995. Femtosecond transient absorption spectroscopy on the light-harvesting Chl a/b protein complex of Photosystem II at room temperature and 12 K. *Chem. Phys.* 194:311–322.

Booth, P. J., and H. Paulsen. 1996. Assembly of light-harvesting chlorophyll a/b complex in vitro. Time-resolved fluorescence measurements. *Biochemistry.* 35:5103–5108.

Brochon, J-C. 1994. Maximum entropy method of data analysis in time-resolved spectroscopy. *In* Methods in Enzymology, Vol. 240. Numerical Computer Methods Part B. M. L. Johnson and L. Brand, editors. Academic Press, San Diego. 262–311.

Cinque, G., R. Croce, A. R. Holzwarth, and R. Bassi. 2000. Energy transfer among CP29 chlorophylls: calculated Förster rates and experimental transient absorption at room temperature. *Biophys. J.* 79:1706–1717.

Connelly, J. P., M. G. Müller, R. Bassi, R. Croce, and A. R. Holzwarth. 1997a. Femtosecond transient absorption study of carotenoid to chlorophyll energy transfer in the light harvesting complex II of photosystem II. *Biochemistry.* 36:281–287.

Connelly, J. P., M. G. Müller, M. Hucke, G. Gatzen, C. W. Mullineaux, A. V. Ruban, P. Horton, and A. R. Holzwarth. 1997b. Ultrafast spectroscopy of trimeric light harvesting complex II from higher plants. *J. Phys. Chem. B.* 101:1902–1909.

Croce, R., G. Cinque, A. R. Holzwarth, and R. Bassi. 2000. The Soret absorption properties of carotenoids and chlorophylls in antenna complexes of higher plants. *Photosynth. Res.* in press.

Croce, R., R. Remelli, C. Varotto, J. Breton, and R. Bassi. 1999a. The neoxanthin binding site of the major light harvesting complex (LHCII) from higher plants. *FEBS Lett.* 456:1–6.

Croce, R., S. Weiss, and R. Bassi. 1999b. Carotenoid-binding sites of the major light-harvesting complex II of higher plants. *J. Biol. Chem.* 274:29613–29623.

Damjanovic, A., T. Ritz, and K. Schulten. 1999. Energy transfer between carotenoids and bacteriochlorophylls in light-harvesting complex II of purple bacteria. *Phys. Rev. E.* 59:3293–3311.

Du, M., X. Xie, L. Mets, and G. R. Fleming. 1994. Direct observation of ultrafast energy-transfer processes in light harvesting complex II. *J. Phys. Chem.* 98:4736–4741.

Eads, D. D., S. P. Webb, T. G. Owens, L. Mets, R. S. Alberte, and G. R. Fleming. 1987. Characterization of the fluorescence decays of the chlorophyll a/b protein. *In* Progress in Photosynthesis Research. 1. J. Biggins, editor. Nijhoff, Dordrecht, The Netherlands. 135–138.

Frank, H. A., J. A. Bautista, J. Josue, Z. Pendon, R. G. Hiller, F. P. Sharples, D. Gosztola, and M. R. Wasielewski. 2000. Effect of the solvent on the spectroscopic properties and dynamics of the lowes excited state of carotenoids. *J. Phys. Chem. B.* 104:4569–4577.

Frank, H. A., V. Chynwat, R. Z. B. Desamero, R. Farhoosh, J. Erickson, and J. Bautista. 1997. On the photophysics and photochemical properties of carotenoids and their role as light-harvesting pigments in photosynthesis. *Pure Appl. Chem.* 69:2117–2124.

Giuffra, E., D. Cugini, R. Croce, and R. Bassi. 1996. Reconstitution and pigment-binding properties of recombinant CP29. *Eur. J. Biochem.* 238:112–120.

Giuffra, E., G. Zucchelli, D. Sandona, R. Croce, D. Cugini, F. M. Garlaschi, R. Bassi, and R. C. Jennings. 1997. Analysis of some optical properties of a native and reconstituted photosystem II antenna complex, CP29: pigment binding sites can be occupied by chlorophyll a or chlorophyll b and determine spectral forms. *Biochemistry.* 36: 12984–12993.

Gradinaru, C. C., S. Özdemir, D. Gülen, I. H. M. van Stokkum, R. van Grondelle, and H. Van Amerongen. 1998. The flow of excitation energy in LHCII monomers: implications for the structural model of the major plant antenna. *Biophys. J.* 75:3064–3077.

Green, B. R., and D. G. Durnford. 1996. The chlorophyll-carotenoid proteins of oxygenic photosynthesis. *Annu. Rev. Plant Physiol. Plant Mol. Biol.* 47:685–714.

Gülen, D., R. van Grondelle, and H. Van Amerongen. 1997. Structural information on the light-harvesting complex II of green plants that can be deciphered from polarized absorption characteristics. *J. Phys. Chem. B.* 101:7256–7261.

Hankamer, B., J. Barber, and E. J. Boekema. 1997. Structure and membrane organization of photosystem II in green plants. *Annu. Rev. Plant Physiol. Plant Mol. Biol.* 48:641–671.

Hobe, S., H. Niemeier, A. Bander, and H. Paulsen. 2000. Carotenoid binding sites in LHCIIb. Relative affinities towards major xanthophylls of higher plants. *Eur. J. Biochem.* 267:616–624.

Horton, P., A. V. Ruban, and R. G. Walters. 1996. Regulation of light harvesting in green plants. *Annu. Rev. Plant Physiol. Plant Mol. Biol.* 47:655–684.

Ide, J. P., D. R. Klug, W. Kühlbrandt, G. Porter, and J. Barber. 1986. Detergent effects upon the picosecond dynamics of higher plant light harvesting chlorophyll complex (LHC). *In* Ultrafast Phenomena V. G. R. Fleming and A. E. Siegman, editors. Springer, Berlin. 406–408.

James, D. R., and W. R. Ware. 1986. Recovery of underlying distributions of lifetimes from fluorescence decay data. *Chem. Phys. Lett.* 126:7–11.

Kleima, F. J., C. C. Gradinaru, F. Calkoen, I. H. M. van Stokkum, R. van Grondelle, and H. Van Amerongen. 1997. Energy transfer in LHCII monomers at 77K studied by sub-picosecond transient absorption spectroscopy. *Biochemistry.* 36:15262–15268.

Kühlbrandt, W. 1994. Structure and function of the plant light-harvesting complex, LHC-II. *Curr. Opinion Struct. Biol.* 4:519–528.

Kühlbrandt, W., D. N. Wang, and Y. Fujiyoshi. 1994b. Atomic model of plant light-harvesting complex by electron crystallography. *Nature.* 367: 614–621.

Kwa, S. L. S., H. Van Amerongen, S. Lin, J. P. Dekker, R. van Grondelle, and W. S. Struve. 1992. Ultrafast energy transfer in LHC-II trimers from the Chl a/b light-harvesting antenna of photosystem II. *Biochim. Biophys. Acta.* 1102:202–212.

Landl, G., T. Langthaler, H. W. Engl, and H. F. Kauffmann. 1991. Distribution of event times in time-resolved fluorescence: the exponential series approach—algorithm, regularization, analysis. *J. Comput. Phys.* 95:1–28.

McTavish, H., R. Picorel, and M. Seibert. 1989. Stabilization of isolated photosystem II reaction center complex in the dark and in the light using polyethylene glycol and an oxygen-scrubbing system. *Plant Physiol.* 89:452–456.

Nussberger, S., J. P. Dekker, W. Kühlbrandt, B. M. van Bolhuis, R. van Grondelle, and H. Van Amerongen. 1994. Spectroscopic characterization of three different monomeric forms of the main chlorophyll a/b binding protein from chloroplast membranes. *Biochemistry.* 33: 14775–14783.

Paulsen, H. 1995. Chlorophyll a/b-binding proteins. *Photochem. Photobiol.* 62:367–382.

Paulsen, H., B. Finkenzeller, and N. Kühlein. 1993. Pigments induce folding of light-harvesting chlorophyll a/b-binding protein. *Eur. J. Biochem.* 215:809–816.

Paulsen, H., and S. Hobe. 1992. Pigment-binding properties of mutant light-harvesting chlorophyll-a/b-binding protein. *Eur. J. Biochem.* 205: 71–76.

Peterman, E. J. G., F. M. Dukker, R. van Grondelle, and H. Van Amerongen. 1995. Chlorophyll a and carotenoid triplet states in light-harvesting complex II of higher plants. *Biophys. J.* 69:2670–2678.

Peterman, E. J. G., C. C. Gradinaru, F. Calkoen, J. C. Borst, R. van Grondelle, and H. Van Amerongen. 1997a. Xanthophylls in light-harvesting complex II of higher plants: light harvesting and triplet quenching. *Biochemistry.* 36:12208–12215.

Peterman, E. J., S. Hobe, F. Calkoen, R. van Grondelle, H. Paulsen, and H. Van Amerongen. 1996. Low-temperature spectroscopy of monomeric and trimeric forms of reconstituted light-harvesting chlorophyll a/b complex. *Biochim. Biophys. Acta.* 1273:171–174.

Peterman, E. J. G., R. Monshouwer, I. H. M. van Stokkum, R. van Grondelle, and H. Van Amerongen. 1997b. Ultrafast singlet excitation transfer from carotenoids to chlorophylls via different pathways in light-harvesting complex II of higher plants. *Chem. Phys. Lett.* 264: 279–284.

Plumley, F. G., and G. W. Schmidt. 1987. Reconstitution of chloroform a/b light-harvesting complexes: Xanthophyll-dependent assembly and energy transfer. *Proc. Natl. Acad. Sci. U.S.A.* 84:146–150.

Porra, R. J., W. A. Thompson, and P. E. Kriedemann. 1989. Determination of accurate extinction coefficients and simultaneous equations for assaying chlorophylls a and b extracted with four different solvents: verification of the concentration of chlorophyll standards by atomic absorption spectroscopy. *Biochim. Biophys. Acta.* 975:384–394.

Prokhorenko, V. I., D. B. Steensgaard, and A. R. Holzwarth. 2000. Exciton dynamics in the chlorosomal antennae of the green bacteria *Chloroflexus aurantiacus* and *Chlorobium tepidum*. *Biophys. J.* 79:2105–2120.

Remelli, R., C. Varotto, D. Sandona, R. Croce, and R. Bassi. 1999. Chlorophyll binding sites of monomeric light harvesting complex (LHCII) reconstituted in vitro: a mutation analysis of chromophore binding residues. *J. Biol. Chem.* 274:33510–33521.

Sandona, D., R. Croce, A. Pagano, M. Crimi, and R. Bassi. 1998. Higher plants light-harvesting proteins. Structure and function as revealed by mutation analysis of either protein or chromophore moieties. *Biochim. Biophys. Acta.* 1365:207–214.

Savikhin, S., H. Van Amerongen, S. L. S. Kwa, R. van Grondelle, and W. R. Struve. 1994. Low-temperature energy transfer in LHC-II trimers from the Chl a/b light-harvesting antenna of photosystem II. *Biophys. J.* 66:1597–1603.

Siemiarczuk, A., B. D. Wagner, and W. R. Ware. 1990. Comparison of the maximum entropy and exponential series methods for the recovery of distributions of lifetimes from fluorescence lifetime data. *J. Phys. Chem.* 94:1661–1666.

Simonetto, R., M. Crimi, D. Sandona, R. Croce, G. Cinque, J. Breton, and R. Bassi. 1999. Orientation of chlorophyll transition moments in the higher-plant light-harvesting complex CP29. *Biochemistry.* 38: 12974–12983.

Trinkunas, G., J. P. Connelly, M. G. Müller, L. Valkunas, and A. R. Holzwarth. 1997. Model for the excitation dynamics in the light-harvesting complex II from higher plants. *J. Phys. Chem. B.* 101: 7313–7320.

Trinkunas, G., M. G. Müller, R. Bassi, L. Valkunas, and A. R. Holzwarth. 1999. Combined modeling of excitation dynamics in LHCII and CP29. *In* Tetrapyrrole Photoreceptors in Photosynthetic Organisms. University of Verona, Verona, Italy.

Trinkunas, G., M. G. Müller, I. Martin, L. Valkunas, and A. R. Holzwarth. 1998. Functional and spectral assignment of chlorophylls in the light harvesting complex II of higher plants. *In* Photosynthesis: Mechanism and Effects/XI. G. Garab, editor. Int. Congr. Photosynthesis Budapest 1998. Kluwer Academic Publishers, Dordrecht, The Netherlands. 285–288.

Ulrych, T. J., and R. W. Clayton. 1976. Time series modeling and maximum entropy. *Phys. Earth Planetary Interiors.* 12:188–200.

Valkunas, L., V. Cervinskas, G. Trinkunas, M. G. Müller, and A. R. Holzwarth. 1998. Excited state mixing effects in transient absorption spectra of photosynthetic light-harvesting complex II. *In* Photosynthesis: Mechanism and Effects/XI. G. Garab, editor. Int. Congr. Photosynthesis Budapest 1998. Kluwer Academic Publishers, Dordrecht, The Netherlands. 281–284.

Valkunas, L., V. Cervinskas, G. Trinkunas, M. G. Müller, and A. R. Holzwarth. 1999. Effects of excited state mixing on transient absorption spectra in dimers. Application to photosynthetic light-harvesting complex II. *J. Chem. Phys.* 111:3121–3132.

Visser, H. M., F. J. Kleima, I. H. M. van Stokkum, R. van Grondelle, and H. Van Amerongen. 1996. Probing the many energy-transfer processes in the photosynthetic light-harvesting complex II at 77 K using energy-selective sub-picosecond transient absorption spectroscopy. *Chem. Phys.* 210:297–312.

Walla, P. J., J. Yom, B. P. Krueger, and G. R. Fleming. 2000. Two-photon excitation spectrum of light-harvesting complex II and fluorescence upconversion after one- and two-photon excitation of the carotenoids. *J. Phys. Chem.* 104:4799–4806.